

Bifurcation analysis of the flight dynamics of a fighter aircraft

Sébastien Kolb

CReA

French Air Force Research Centre, BA 701, 13661 Salon Air, France

sebastien.kolb@defense.gouv.fr

Abstract

The flight dynamics of a fighter aircraft is highly nonlinear. By means of bifurcation theory, such non-linear behaviours will be examined and explained. In this work, the flight dynamics of the F-18 aircraft is analyzed. The longitudinal flights and turns reveal to be simple flight phases for which bifurcations and abrupt events occur such as the appearance of multiple equilibria or periodical orbits. The nonlinear analysis is helpful to warn against unexpected situations and to understand the underlying physics. The couplings between aircraft and pilot are also subject to some flying qualities cliffs which will be examined.

Introduction

After presenting the existing F-18 HARV model, some flight phases will be analyzed like longitudinal flights or turns and also the pilot-aircraft couplings. The bifurcations which are observed give rise to unexpected behaviours which can be harmful. But their analysis allows to predict them correctly and to react more adequately.

1. Modelling

The F-18 HARV aircraft model used here is the one furnished in the article¹ and the associated matlab code² is available on internet. A classical flight dynamics model is adopted that is to say $\dot{X} = f(X, U)$ where the state vector $X = \{Mach, \alpha, \beta, p, q, r, \phi, \theta\}$ and the control vector $U = \{thr, \delta_e, \delta_r, \delta_a\}$. The altitude is fixed at sea level as simplifying assumption.

A huge work on the flight dynamics analysis of a F-18 HARV was already performed like in the articles³ of N.K. Sinha. The focus of this study is here put on some particular flight dynamics phases. Besides in order to study the differential equations, the calculations are performed with the *matcont*⁴ toolbox. A link is made between the mathematics of bifurcation theory⁵ and flight dynamics⁶ like in other similar studies.¹⁰

2. Longitudinal flight

In this section, the longitudinal flight is studied that is to say only the flight in the vertical plane is considered and there are zero sideslip β and no transverse rotations ($p = 0, r = 0$), all the forces are in the longitudinal vertical plane and all the moments are orthogonal to this plane.

Such a flight involves the two controls of elevator deflection and throttle $U = \{\delta_e, thr\}$ and the longitudinal state variables. The figure 1 presents the angles-of-attack α at equilibrium (and in limit cycles) versus elevator deflection δ_e with a fixed throttle (during climb, level flight and descent) $thr \approx 40\%$. A Hopf bifurcation⁵ is seen at $\delta_e \approx -14.9^\circ$ where periodical orbits are appearing suddenly which may surprise the pilot. This can be a hazardous situation to manage (especially with a nonzero flight-path angle).

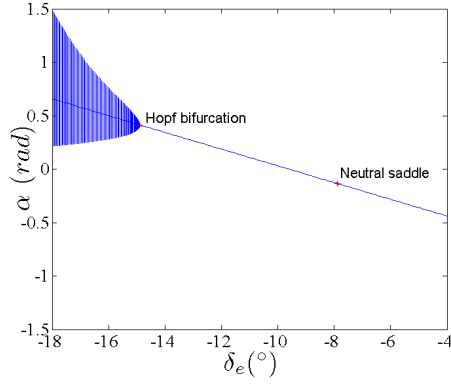


Figure 1: Bifurcation diagram for a pure longitudinal flight of the F-18 HARV aircraft

At the Hopf bifurcation, the pair of complex conjugate eigenvalues associated is $\lambda_H = \pm 0.257i$ that is to say a period $T_H = 24.5$ s. The eigenvector components and the state values are given in the table 1.

	eigenvector	equilibrium
<i>Mach</i>	$0.0086 \pm 0.0499i$	0.149
α	$0.298 \pm 0.563i$	0.414
β	0	0
p	0	0
q	$-0.216 \pm 0.283i$	0
r	0	0
ϕ	0	0
θ	0.682	0.225

Table 1: Hopf bifurcation

Thus the loss of phugoid stability is responsible for this Hopf bifurcation. Effectively the period verifies $T_H \approx \frac{\pi\sqrt{g}}{g} \times \text{airspeed} = T_{\text{phugoid}}$ from classical flight dynamics textbook⁶. There is a negative flight-path angle $\gamma = \theta - \alpha = -0.188$ rad.

Normally a phugoid mode can become unstable due to propulsion or a flight-path angle higher than $\gamma_{crit} = \arcsin \frac{2}{f}$ in a climb phase or even due to Mach effect in transonic regime. But here it seems due to stall effect.

Moreover the critical controls (elevator deflection δ_e and throttle *thr*) for which a bifurcation occurs are plotted in the figure 2. It shows Hopf bifurcations and branch points.

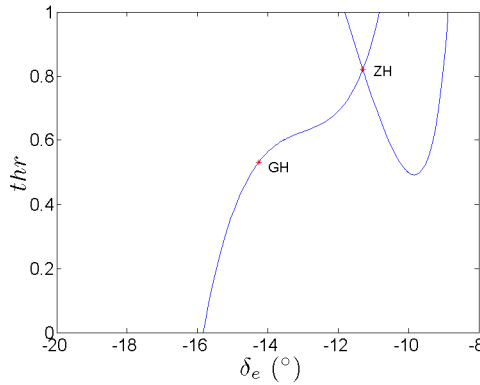


Figure 2: Locus of the bifurcation points in the (δ_e, thr) plane

The global Hopf bifurcation at the critical parameters $thr \approx 53\%$, $\delta_e \approx -14.3^\circ$ changes the way periodical orbits are created i.e. for lower or higher elevator deflections than the bifurcation value like shown in figure 3.

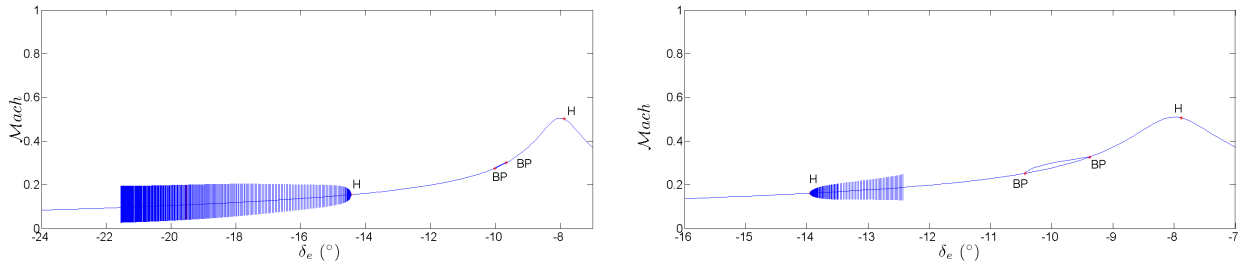


Figure 3: Bifurcation diagram with elevator deflections δ_e as parameter and periodical orbits created by the Hopf bifurcation for throttle $thr = 50\%$ (left) and $thr = 60\%$ (right)

For a throttle $thr = 0.6$, the (stable) limit cycles appear for higher elevator deflections than the critical one and the so-called first Lyapunov calculated by *matcont* is positive that is to say the Hopf bifurcation is *subcritical* whereas for a throttle $thr = 0.5$, the (stable) limit cycles appear for lower elevator deflections than the critical one and the so-called first Lyapunov calculated by *matcont* is negative that is to say the Hopf bifurcation is *supercritical*.

Besides in figure 2, the Zero Hopf bifurcation at $thr \approx 82\%$, $\delta_e \approx -11.3^\circ$ indicates a new phenomenon. There is a range of elevator deflections ($\delta_e \in [-12^\circ, -9^\circ]$, $thr \geq 50\%$) for which multiple equilibria coexist due to branch points. It changes the instinctively predicted behaviour due to an elevator deflection modification (in comparison with a classical linear evolution) such that more attention is required from the pilot.

For the next calculations, the throttle is fixed at $thr = 70\%$ and the elevator deflection δ_e is varied. A classical result of flight dynamics is that for one elevator angle, there is only one equilibrium and especially one angle-of-attack. But for this F-18 aircraft, several critical behaviours are observed in figure 4.

The figure 4 is the bifurcation diagram associated to the longitudinal flight and represents the bank angle ϕ at equilibrium in function of the elevator deflection δ_e for a throttle $thr \approx 70\%$. A region where there are two stable (nonzero) bank angles and one unstable (zero) bank angle is visible.

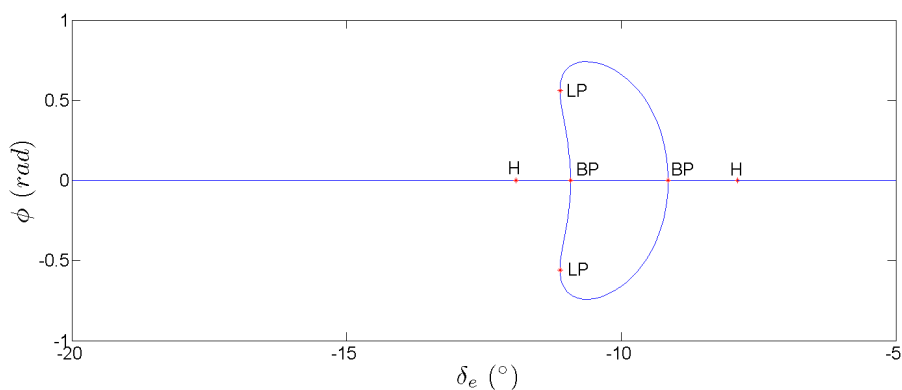


Figure 4: Bifurcation diagram for the longitudinal flight of a F-18 aircraft with a throttle $thr \approx 70\%$

On the one hand, as seen before, the Hopf bifurcation at the elevator deflection $\delta_e \approx -11.9^\circ$ involves the variables $(Mach, \alpha, q, \theta)$ and is associated to the (pair of complex conjugate) eigenvalues $\lambda_H = \pm 0.298i$ and the phugoid mode. The aircraft begins suddenly to oscillate at a flight path angle of $\gamma = 3.7^\circ$ after this destabilization.

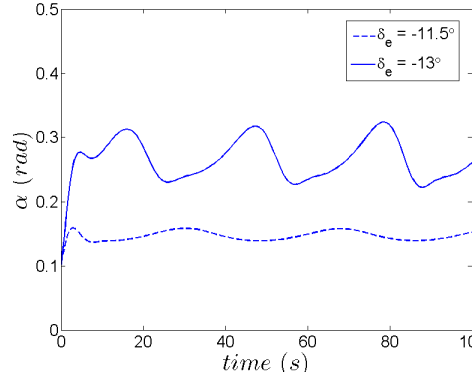


Figure 5: Time simulations for elevator deflections higher or lower than the critical Hopf bifurcation value

The figure 5 shows the behaviour for elevator deflections higher or lower than the critical Hopf bifurcation value. A stable limit cycle exists when $\delta_e = -13^\circ$.

On the other hand, the branch point at the elevator deflection $\delta_e \approx -10.9^\circ$ involves the variables (β, p, r, ϕ) and is associated to the eigenvalue $\lambda_{BP} = 0$ and the spiral mode (as observed in figure 6). That's why from this equilibrium point, it is possible to have stable equilibria with nonzero bank angle. It changes the way the aircraft behaves in turn since it can stabilize itself in such a situation without any action of the lateral controls. The pure longitudinal flight is unexpectedly lost.

Moreover between the two branch points linked to elevator deflections $\delta_e = -9.1^\circ$ and $\delta_e = -10.9^\circ$, the classical longitudinal equilibrium becomes unstable. The aircraft may stabilize at a nonzero bank angle. The bifurcations occur respectively for flight-path angle of respectively $\gamma \approx 5.8^\circ$ (climb) and $\gamma \approx -10.3^\circ$ (descent). This fact is shown in the time simulations figure 6 where for an initial bank angle $\phi = -0.3 \text{ rad}$, the asymptotic value of ϕ is not the same for elevator deflections of $\delta_e = -12^\circ$ or $\delta_e = -10.5^\circ$.

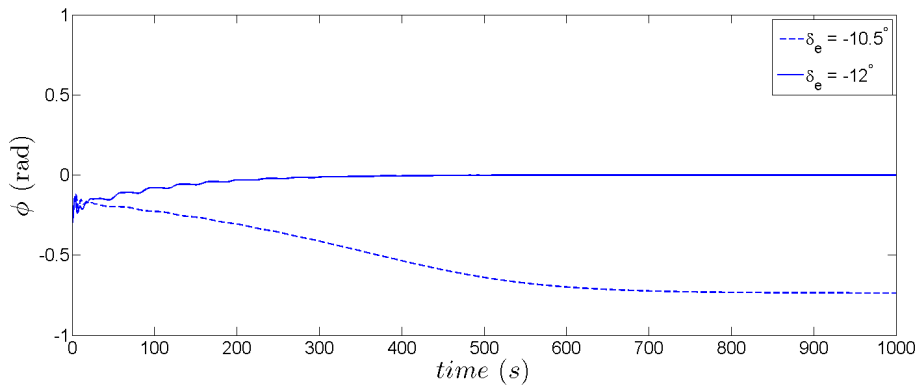


Figure 6: Time simulations for elevator deflections between or outside the critical branch point values

A little action on the elevator implies a stabilization at a nonzero bank angle which can be recovered by an adverse action (reversibility). It is nevertheless a very astonishing behaviour for an aircraft although the spiral motion is very low and thus easier to counteract.

The branch points occur for $\alpha \approx 0.1 \text{ rad} \approx 5.8^\circ$ and $\alpha \approx -0.037 \text{ rad} \approx -2.1^\circ$. In the terminology of bifurcation theory,⁵ these last ones are so-called pitchfork bifurcations. The analysis of the eigenvalues and eigenvectors (components furnished in table 2) shows that the spiral mode is responsible for the appearance of these bifurcations and of the coexistence of several equilibria with different bank angles. We can use the classical stability criterion of the spiral mode to identify this behavior that is to say $C_{l\beta}C_{nr} > C_{lr}C_{n\beta}$. The question is whether too much route stability $C_{n\beta}$ or too little dihedral effect $C_{l\beta}$ is responsible for the destabilization of the spiral mode.⁶ Considering the values of the Jacobian matrix for different equilibria, it seems that at the branch point, there is too much route stability $\frac{\partial \dot{r}}{\partial \beta} \propto C_{n\beta} (>> 0)$ and too much induced roll $\frac{\partial \dot{p}}{\partial r} \propto C_{lr} (>> 0)$.

For the branch point occurring at $\delta_e \approx -10.9^\circ$ and linked to a zero eigenvalue, the state variable values and the associated eigenvector are given in the table 2.

	eigenvector	equilibrium
<i>Mach</i>	0	0.233
α	0	0.097
β	0.0229	0
p	-0.0214	0
q	0	0
r	0.1157	0
ϕ	0.9928	0
θ	0	0.177

Table 2: Branch point

Both behaviours may surprise the pilot and make him react unadequately or too late in order to cope with this unusual situation such that it may increase the hazardousness of such a situation.

After studying the longitudinal flight for which some unexpected bifurcations were diagnosed and whose consequences (periodical orbits, multiple equilibria) were analyzed, the next section will deal with aircraft turns.

3. Turns

In order to engage a turn, the controls of rudder and ailerons can be used. Both maneuvers are performed and the associated equilibria are calculated. It would have been interesting also to study the coordinated turns, but this is not accomplished here. At the end, the pilotability of the bank angle is also assessed.

3.1 Rudder

Firstly, the rudder deflection is varied as shown in figure 7. At a rudder deflection of $\delta_r \approx 20^\circ$, a bifurcation occurs which implies a jump as shown by both bifurcation diagram and time simulations for $\delta_r = -19^\circ$ and $\delta_r = -21^\circ$ in the figure 7. Indeed with a little modification of the rudder deflection δ_r , the stabilized yaw rate r is highly increased.

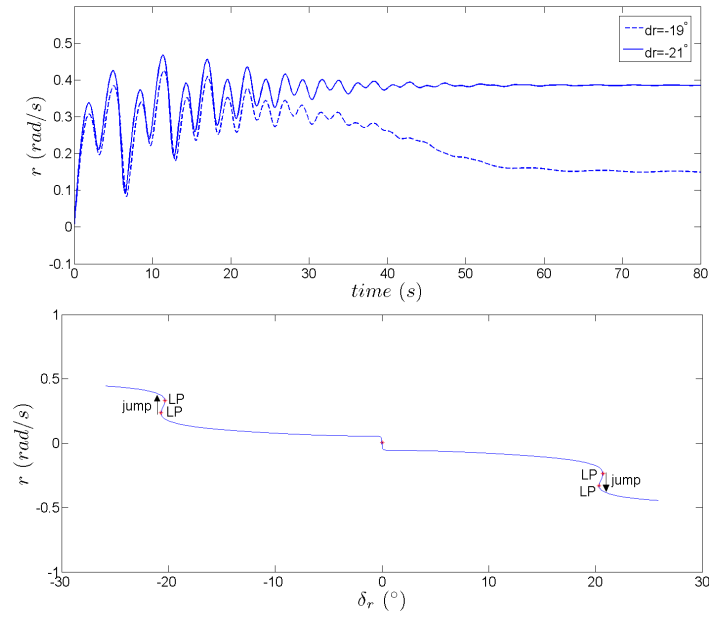


Figure 7: Bifurcation diagram linked to a turn made simply with the rudder and time simulations for different rudder deflections

When performing such a turn at the limit of the rudder authority, the pilot must be careful since remaining in such a flight situation for a long time may lead to a hazardous yaw rate. Concerning the effectiveness of the rudder, we can say that a limitation appears in its use due to the nonlinear behaviour of the flight dynamics. As a partial conclusion, we can state that the *effective* physical limitation of the rudder is lower than the mechanical one.

3.2 Ailerons

Secondly the aileron deflection is also varied to perform a turn. For huge aileron deflections, when the throttle is fixed at $thr = 0.5$ and the elevator deflection at $\delta_e = -15^\circ$, there is also a jump of roll rate near $\delta_a = \pm 32^\circ$ which is illustrated in the figures 8 and 9. Contrary to this situation, at an aileron deflection $\delta_a = \pm 18^\circ$, the high roll rate may suddenly disappear.

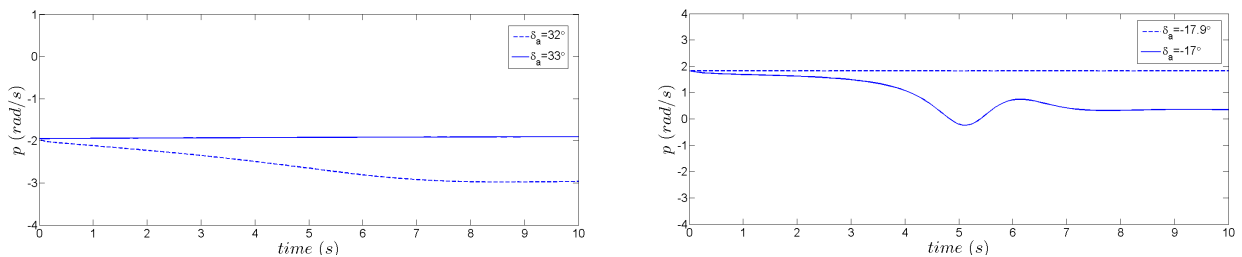


Figure 8: Time simulations for different aileron deflections: $\delta_a = 32^\circ, \delta_a = 33^\circ$ (left) and $\delta_a = -17.9^\circ, \delta_a = -17^\circ$ (right)

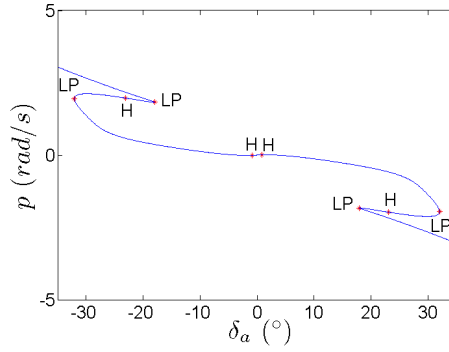


Figure 9: Bifurcation diagram with aileron deflection δ_a as parameter

Finally these simple maneuvers of turn seem to give rise to unexpected behaviour due to the nonlinear behaviour of the aircraft. As a recommendation, for practical use, it is advisable not to use lateral control of rudder and ailerons near their mechanical limits since high bank angles and roll rates are predicted.

Since we know that there may be some problems with the lateral controls, we look in the next section how well it is possible to pilot the bank angle with the ailerons.

3.3 Roll

We can look at the effect of aileron deflection on the bank angle ϕ . In the bifurcation diagrams (figure 10) with aileron deflection δ_a , a linear variation is observed near the neutral position, but bifurcations and especially limit points imply a sudden huge change of bank angle and even a jump. It can be dangerous if the pilot is not aware of this fact.

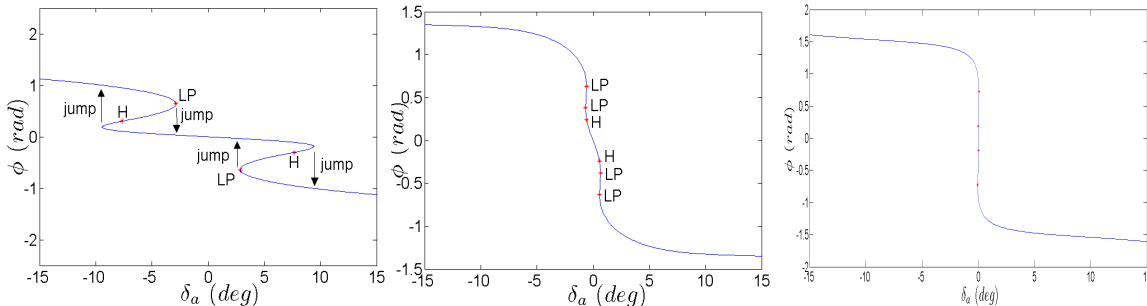


Figure 10: Bifurcation diagram with aileron deflection δ_a as parameter and elevator deflection $\delta_e = -16.1$ deg, $\delta_e = -14.45$ deg and $\delta_e = -11.6$ deg

On the contrary, for $\delta_e \geq -11.6$ deg (high speeds), the jump is immediate and no linear region is observable, the roll command acts as a three-state command. These constatations are helpful to notice in order to know in advance when it is necessary to pay attention and when things are more natural.

To put in a nutshell, the range of elevator deflections for which ailerons are effective and usable in a sensible manner is quite reduced.

The bare F-18 HARV aircraft was studied in the previous sections and reveals some unexpected behaviours such as the existence of periodical orbits, multiple equilibria and jumps which were analyzed thanks to the bifurcation theory. Nevertheless the pilot may also have an impact on the overall aircraft behaviour. The next section uses nonlinear dynamical system theory in order to examine these couplings.

4. Pilot-in-the-loop

The pilot-in-the-loop may impact greatly the flight dynamics in the sense that the pilot may change by his reaction the global aircraft behaviour. This section will deal with the topic of pilot induced oscillations due to rate limiting.

Pilot induced oscillations consists in sustained or uncontrollable oscillations resulting from the efforts of the pilot to control the aircraft i.e. critical phase difference between the pilot action on the controls and the aircraft response. Here we are dealing with the consequences of rate limiting that is to say mainly a jump in phase once the limitation in rate is reached. From the theoretical point of view, it's a PIO of category II.

The methodology employed here for the analysis of pilot-induced-oscillations is based on the OLOP criterion⁷ of DLR (Deutsches Zentrum für Luft-und-Raumfahrt) and on the examples furnished in the projects of GARTEUR⁸ and AGARD.⁹

The basic effects of a rate saturation can be assessed with the describing function method. This quasi-linear approximation shows a huge increase in phase when the rate limiter becomes active. In a command channel, this can provoke a critical global delay and lead to pilot-aircraft couplings.

The different steps to perform so as to determine the OLOP criterion consist in the calculation of a:

1. simple gain pilot model (using the "crossover model" or "synchronous precognitive behaviour") based on linear aircraft dynamics and verifying $K_{pilot}(\Phi_{cr}) \cdot |F_{open-loop aircraft}(\omega_{cr})| = 1 (0dB)$
2. linear closed loop frequency response from stick input to the input to the rate limiter
3. Closed Loop Onset Frequency $\hat{\omega}_{onset}: \hat{u}_c \cdot |F_{u_c}^{u_{rie}}| = \frac{R}{\hat{\omega}_{onset}}$
4. required open-loop frequency response, separation into amplitude $A_0(\omega)$ and phase angle $\Phi_0(\omega)$
5. Open Loop Onset Point location compared to OLOP boundary [$\Phi_0(\hat{\omega}_{onset}), A_0(\hat{\omega}_{onset})$]

Moreover the lateral flight command channel correspond to the *simulink* file of the figure 11 where there is an aileron rate limit.

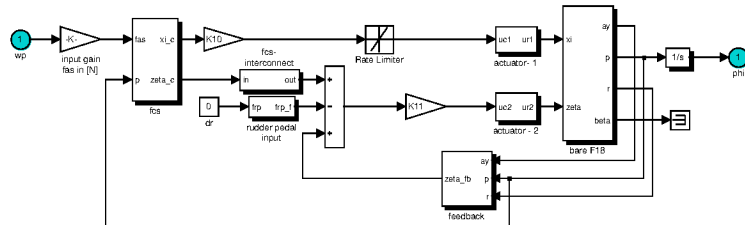


Figure 11: F-18 lateral command channel

These events are linked to bifurcation of limit cycles or transformation of a stable equilibrium into a limit cycle (Hopf bifurcation) due to a sudden jump (mainly in phase) consecutive to the activation of the rate saturation. The dangerousness of these jumps are delimited by the OLOP frontier.

For diverse type of pilots ($\Phi_{cr} = -110^\circ$ corresponds to a cool pilot, $\Phi_{cr} = -160^\circ$ corresponds to a very aggressive pilot), the results of the analysis are given in the table 3.

	$R = 90^\circ/s$	$R = 130^\circ/s$	$R = 170^\circ/s$	$R = 210^\circ/s$
$\Phi_{cr} = -110^\circ$	No PIO	No PIO	No PIO	No PIO
$\Phi_{cr} = -120^\circ$		No PIO	No PIO	No PIO
$\Phi_{cr} = -130^\circ$	PIO	No PIO	No PIO	No PIO
$\Phi_{cr} = -140^\circ$	PIO	PIO	No PIO	No PIO
$\Phi_{cr} = -150^\circ$	PIO	PIO		No PIO
$\Phi_{cr} = -160^\circ$	PIO	PIO	PIO	No PIO

Table 3: Susceptibility to PIO as predicted by the OLOP criterion in function of pilot aggressiveness and rate limit

The dangerousness of the pilot-aircraft couplings due to a rate limited actuator (aileron) is assessed thanks to the describing function method and the OLOP criterion. The susceptibility of the F-18 aircraft to PIO and the tolerable rate limitations are evaluated.

Conclusion

This study allows to understand the flight dynamics of a F-18 fighter aircraft whose model is taken "as is". It analyzes what happens and predicts some potentially harmful events by making the links between the flight dynamics and the mathematics of nonlinear dynamical system. Unexpected Hopf and pitchfork bifurcations appear suddenly in the longitudinal flight giving rise respectively to periodical orbits and multiple equilibria. Effective limitations of the lateral controls were also diagnosed due to jump phenomena. The role of the aggressive pilot in the excitation of a rate limited actuator in a flight command channel was also shown.

As perspectives, in further work, more complicated flight types and phenomena met by a fighter aircraft can be analyzed. The flight model can possibly also be improved.

References

- [1] Frederick H. Lutze Yigang Fan and Eugene M. Cliff. Time-optimal lateral maneuvers of an aircraft. *Journal of Guidance, Control, and Dynamics*, 18(5):1106–1111, 1995.
- [2] Anshu Narang. Project: To simulate behaviour of the f-18 harv. <https://canvas.uw.edu/courses/986601/assignments/3016170>, 2014. Advanced Dynamics, Validation & Control Research Laboratory, University of Washington, Seattle.
- [3] N.K. Sinha. Application of bifurcation methods to f-18/harv open-loop dynamics in landing configuration. *Defense Science Journal*, 52(2), 2002.
- [4] A. Dhooge, W. Govaerts, and Yu. A. Kuznetsov. Matcont: A matlab package for numerical bifurcation analysis of odes. *ACM Trans. Math. Softw.*, 29(2):141–164, 2003.
- [5] J. Guckenheimer and P. Holmes. *Nonlinear Oscillations, Dynamical Systems and Bifurcations of Vector Fields*. Springer, 2002.
- [6] B. Etkin and L.D. Reid. *Dynamics of Flight: Stability and control*. John Wiley & Sons, Inc., 3rd edition, 1996.
- [7] H. Duda. Prediction of pilot-in-the-loop oscillations due to rate saturation. *Journal Of Guidance, Control, And Dynamics*, 20(3), mai-juin 1997.
- [8] FM(AG12). Analysis of nonlinear pilot-vehicle systems using modern control theory. Technical Report TP-120-02, GARTEUR, 2000.
- [9] AGARD. *Flight Control Design - Best Practices*. Number RTO-TR-029. North Atlantic Treaty Organization, 2000.
- [10] M.G. Goman, G I. Zagainov, and A.V. Khramtsovsky. Application of bifurcation methods to nonlinear flight dynamics problem. *Progress in Aerospace Scineces*, 33:539–586, mars 1997.